European Polymer Journal 221 (2024) 113551

Contents lists available at ScienceDirect

European Polymer Journal

journal homepage: www.elsevier.com/locate/europolj

Frontal polymerization of acrylamide/GelMA/gelatin hydrogels with controlled mechanical properties and inherent self-recovery

Luana Di Lisa [a,1], Mariangela Rea [a,1], Daniele Nuvoli [b,*], Maria Letizia Focarete [a,c,**], Cristiano Albonetti [d], Alberto Mariani [b]

[a] Department of Chemistry 'Giacomo Ciamician' and INSTM UdR of Bologna, University of Bologna, via Selmi 2, 40126 Bologna, Italy
[b] Department of Chemical, Physical, Mathematical and Natural Sciences, University of Sassari, and local INSTM Unit, via Vienna 2, 07100 Sassari, Italy
[c] Interdepartmental Center for Industrial Research in Health Sciences and Technologies, University of Bologna, Via Tolara di Sopra, 41/E, 40064 Ozzano Emilia, Bologna, Italy
[d] Consiglio Nazionale delle Ricerche – Institute for the Study of Nanostructured Materials (CNR-ISMN), Via P. Gobetti 101, 40129 Bologna, Italy

ARTICLE INFO

Keywords:
Frontal polymerization
Hydrogels
Gelatin
Gelatin methacrylate
Self-recovery
Semi-IPN

ABSTRACT

Low mechanical resistance represents one of the significant problems of hydrogels, limiting their applicability in many fields. One approach to overcome this issue is synthesizing interpenetrating polymeric networks. In this work, the frontal polymerization technique was used to synthesize two series of novel hydrogels: (i) poly (acrylamide) (PAAm)-based hydrogels copolymerized/crosslinked with methacrylate gelatin (GelMA) (AAm-GelMA copolymer networks), and (ii) semi-IPN made of AAm-GelMA copolymer networks and a physically crosslinked gelatin network. With the final objective of improving the rheological, mechanical, morphological, thermal, and swelling properties of PAAm hydrogels, GelMA with two different degrees of methacrylation (30 and 75 mol%) was used. Interactions between GelMA chains, which give rise to physical network formation (i.e., GelMA-GelMA interactions), resulted in very efficient crosslinking for PAAm-based hydrogels, requiring a significantly lower methacrylic group concentration (0.04 mol%) for hydrogel formation compared to N,N′-methylene-bis-acrylamide (1 mol%), which is the agent typically used as a crosslinker for PAAm. Furthermore, the degree of GelMA methacrylation markedly affected the properties of the hydrogels. For example, regarding the swelling degree, hydrogels containing 22 wt% of GELMA30 had an SR% of 2870, while those containing the same amount of GELMA75 swelled much less (870 %). The introduction of gelatin as a secondary network in semi-IPNs influenced the rheological and mechanical properties, resulting in increased hydrogel modulus and stiffness attributed to enhanced physical interactions within the network. Finally, dynamic rheological shear strain and cyclic loading compression tests demonstrated exceptional recovery capabilities in all hydrogel formulations: samples subjected to alternating low (0.1 %) and high (300 % or 10 %) shear strain demonstrated a complete and prompt recovery of G′ and G″ values.

1. Introduction

Hydrogels, three-dimensional (3D) hydrophilic networks composed of crosslinked macromolecular chains capable of holding a large amount of water, are a class of polymeric materials renowned for their versatility and wide-ranging applications, such as drug release, sensors, and tissue engineering devices [1]. The low mechanical resistance represents one of the significant problems of hydrogels that limits their applicability in many fields. To address this issue, the most common approaches that have been proposed include the synthesis of interpenetrated networks [2] and reinforcement with micro or nanoparticles [3]. Polyacrylamide (PAAm), a widely employed polymer, serves as a foundational material for various crosslinked structures. Its chemical stability, tunable mechanical properties, high swelling degree, and optical transparency have allowed this polymer to be widely used in applications in the biomedical field, such as the fabrication of contact lenses [4], tissue engineering [5], and drug delivery [6]. Nonetheless, limitations in mechanical properties and the complexity of synthesis methods hinder the full potential of

* Corresponding author.
** Corresponding author at: Department of Chemistry 'Giacomo Ciamician' and INSTM UdR of Bologna, University of Bologna, via Selmi 2, 40126 Bologna, Italy.
E-mail addresses: dnuvoli@uniss.it (D. Nuvoli), marialetizia.focarete@unibo.it (M.L. Focarete).
[1] These authors contributed equally.

https://doi.org/10.1016/j.eurpolymj.2024.113551
Received 8 August 2024; Received in revised form 30 October 2024; Accepted 3 November 2024
Available online 4 November 2024

PAAm hydrogels in various applications. An efficient method to solve these problems is to introduce thermoreversible and rigid components into the PAAm network [7]. Gelatin is a natural polymer derived from the hydrolytic degradation of collagen, with high potential for biomedical applications [8]. It can form a physically entangled network, thanks to establishing hydrogen bonds among the lateral groups of amino acid sequences. However, gelatin's physical hydrogel is not stable at 37 °C (i.e., the physiological temperature), above which it acts as a liquid. Therefore, The exploitation of this material for tissue engineering or biomedical applications is impossible. To overcome this drawback, gelatin has often been blended with synthetic polymers, such as polyvinyl alcohol (PVA) [9,10], and is deeply characterized in mechanical and biological properties for tissue engineering applications. Another approach that allows for the exploitation of the favorable biological properties of gelatin is chemical modification. It can be performed to form covalent lateral bonds among the polymeric chains and make the network more stable. A simple and inexpensive method to do so is represented by the preparation of GelMA (methacrylate gelatin), which consists of adding side methacrylic groups to the gelatin backbone, which can be exploited for photocrosslinking in the presence of a proper photoinitiator and upon UV light exposure [11]. Thanks to covalent bonds, the network also becomes stable at higher temperatures. GelMA can mimic critical characteristics of the native extracellular matrix (ECM) by incorporating the cell-attaching motifs into the macromolecular chain, favoring cell proliferation and spreading. Despite their advantages, biocompatible/biodegradable hydrogel formulations based on gelatin or GelMA exhibit deficiencies in mechanical properties since they permanently deform and break under repeated compressive loading; thus, there is a critical need for highly elastic, robust hydrogels to progress this mechanistic-modulation strategy in the tissue engineering field.

To improve this aspect, various copolymers containing both biopolymers and synthetic polymers have been synthesized over the years [12]. For example, the copolymerization of methacrylate gelatin with acrylamide has led to the obtaining of hydrogels with superior properties compared to their homopolymers. Serafim et al. [13] and Han et al. [14] investigated GelMA – polyacrylamide copolymers synthesized by a one-pot UV method that showed enhanced compression strength, improved elasticity, and a favorable degradation rate compared to polyacrylamide hydrogels. Moreover, Molino et al. [15] prepared GelMA-acrylamide copolymer networks with improved UV crosslinking and mechanical properties for 3D biofabrication, while Abdallah et al. [16] studied GelMA-AAm hydrogels in which the mechanical and swelling properties are modulated depending on the polymer/water concentration.

Traditional hydrogels are synthesized using classical thermal or UV polymerization reactions, often requiring complex reaction routes, long times, and high energy consumption. The frontal polymerization (FP) technique [17,18] represents an alternative strategy to limit the drawbacks associated with the synthesis of polymeric hydrogels [19]. FP is a self-sustaining reaction technique triggered by an initial stimulus (e.g., thermal or photo), generating a localized reaction zone, the so-called "polymerization front." In FP, the heat released by the exothermic polymerization in this zone provides a sufficient temperature increase to initiate additional polymerization events at the boundary between polymer and unreacted monomer phases, often resulting in stable propagation. Compared to batch polymerization, FP has a more straightforward reaction route, shorter time, and lower energy consumption. FP has been widely used to obtain several types of hydrogels [19–22].

In recent years, semi-interpenetrating polymer networks (semi-IPNs) and interpenetrating polymer networks (IPNs) have emerged as innovative materials, especially in biomedical and pharmaceutical applications [23]. An IPN involves two or more independent networks, either fully or partially interlaced on a molecular scale without covalent bonds [24]. An IPN is composed of two independent polymers with different chemical compositions. If one polymer is linear and penetrates another crosslinked network without any chemical bonds between them, the resulting material is called a semi-IPN. Compared to single network hydrogels, the main advantages of these materials are that relatively dense hydrogel matrices can be produced, which feature stiffer and more rigid mechanical properties, more widely controllable physical properties, and more efficient drug loading [25]. Razmjooee et al. [26] reported the synthesis of Gelatin/Polyacrylamide/Carboxymethyl chitosan triple-network hydrogels with tunable mechanical properties according to the crosslinking agent concentration. They also demonstrated adequate cell viability, non-toxicity, and a suitable proliferation rate of the realized hydrogel systems. A recent work by Goudarzi and Saber-Samandari [27] described the synthesis of polyacrylamide/gelatin/alginate multiple-networks hydrogels through photopolymerization. The influence of N,N′-methylene-bis-acrylamide concentration as a crosslinking agent on hydrogels intended for wound dressings was studied, resulting in adjustable mechanical properties and swelling capacities.

Improving homogeneity and incorporating energy dissipation mechanisms have been recognized as effective methodologies to enhance the mechanical performance of hydrogels [28]. The toughness of the hydrogels can be tuned if the semi-IPN or the IPN contains two types of independent networks, a rigid network and a flexible network, which makes these hydrogels suitable for load-bearing tissues. In past years, we investigated the possibility of obtaining semi-IPN and IPN through FP. For example, semi-IPN based on crosslinked poly(N-isopropylacrylamide) and methylcellulose [29], crosslinked PAAm and methylcellulose [30], and IPN based on poly(N-isopropylacrylamide), 2-hydroxyethyl methacrylate, and 2-acrylamido-2-methylpropanesulfonic acid [31] were reported. Several IPN and semi-IPN polymer systems containing acrylamide and gelatin have recently been studied. For example, Ruvacalba et al. [32] investigated the effect of pH and gelatin concentration on the swelling kinetics and mechanical properties of AAm-gelatin semi-IPN. At the same time, Xiaoqiang et al. studied IPN double networks based on gelatin and polyacrylamide with high strength, self-recovery, and self-healing properties [33]. Moreover, Fan et al. studied various shape memory polyacrylamide/gelatin (PAAm-Gel) hydrogels with interpenetrating double networks synthesized via a one-pot method involving UV [34], and Baojiang et al. [35] investigated the obtainment of Gelatin/PAAm IPN double network hydrogels with super compressibility. However, in these studies, the acrylamide was crosslinked using N,N'-methylene-bis-acrylamide.

The improvement of the properties of PAAm when it is copolymerized with GelMA suggested that we investigate the possibility of obtaining semi-IPN hydrogels based on acrylamide and gelatin, in which the former is crosslinked/copolymerized with GelMA. Besides the improvements deriving from the obtained semi-IPN networks, this work has also exploited the physical interactions (hydrogen bonds) that are established between the two networks due to amino acid groups present both in GelMA (first network) and gelatin (second network). Having as the final objective the improvement of the rheological, mechanical, thermal, and swelling properties of PAAm hydrogels, GelMA was used with two different degrees of methacrylation (30 and 75 mol%) to obtain both copolymers with acrylamide and semi-IPNs in which a second gelatin network is present. Namely, we studied the effect of introducing GelMA and a second gelatin network. The polymerization technique represents another novelty of this work: we demonstrate that methacrylate gelatin systems can be polymerized using FP instead of the classic UV polymerization.

2. Materials and methods

2.1. Materials

Acrylamide (AAm, purity ≥ 98 %), N,N′-methylene-bis-acrylamide (BIS, purity ≥ 99 %), Type A gelatin from porcine skin (gel strength

~300 g Bloom), methacrylic anhydride (MAA) (94 %), ammonium persulfate (APS, purity ≥ 98 %), dialysis cellulose membrane (12–14 kDa cutoff avg. flat width 25 mm) (94 %) were purchased from Sigma-Aldrich®, and dimethyl sulfoxide (DMSO, purity ≥ 99.5 %) was purchased from VWR®.

2.2. Gelatin methacrylate (GelMA) synthesis

GelMA hydrogels with two different methacrylation degrees (MD) were synthesized following previously optimized procedures [36]. In brief, 20 g of gelatin (10 % w/v) were dissolved in a carbonate-bicarbonate buffer (0.25 M, pH 9). Subsequently, MAA (2 ml and 2.5 μL for a methacrylation degree of 75 % and 25 %, respectively) was introduced into the gelatin solution under vigorous stirring (500 rpm) at 50 °C. As the reaction initiated, the generation of methacrylic acid sub-products led to a decrease in pH. To facilitate the methacrylation process, 5 M NaOH was added to the reaction mixture to maintain the pH at 9. After 1 h, the reaction was quenched by gradually adding 37 % v/v HCl until reaching pH 7.4. To eliminate the methacrylic acid sub-products, the mixture underwent dialysis for five days at 37 °C with gentle stirring against ultrapure water (Milli-Q-H_2O). The resulting dialyzed GelMA solution was subjected to freeze-drying and stored at -4 °C. The obtainment of gelatin methacrylate with a MD of 75 % (GelMA75) or 30 % (GelMA30) was confirmed by 1H NMR spectrometry, according to the method reported in the literature [37]. Analyses were performed on a Bruker Advance III 400 spectrometer using 20 mg GelMA dissolved in 0.70 mL D_2O. The new signals at $\delta = 5.4$ and 5.7 ppm, which correspond to the acrylic protons of methacrylic groups of the methacrylic anhydride structure, validate the synthesis. The methacrylation degree was calculated by considering the decrease in intensity of the arginine methyl group signal at 2.85 ppm, using equation (1).

$$\text{Methacrylation degree (mol\%) or MD} = 1 - \frac{\text{integration signal of arginine from GelMA}}{\text{integration signal of arginine from Gelatin}} \cdot 100 \quad (1)$$

2.3. Synthesis of hydrogels through Frontal Polymerization

As regards the synthesis of AAm-GelMA copolymer networks, the desired amount of GelMA30 or GelMA75 (0.125, 0.625, 1.250, or 1.880 g, see Table 1) was gradually added to 10 g of DMSO. This operation was performed using an ultrasonic bath (power = 0.55 kW) with a water temperature of 50 °C to improve the solubilization process. The mixture was cooled to room temperature, and 4.420 g of AAm were then added and dissolved to obtain a homogeneous solution. Lastly, the initiator APS (0.25 mol% with respect to AAm) was added. For semi-IPN synthesis, 1.250 g of GelMA30 (0.04 mol% with respect to AAm) or GelMA75 (0.10 mol% with respect to AAm) were gradually dissolved in 10 g of DMSO. Then, the desired quantity of gelatin (0.220, 0.440, or 1.450 g, see Table 1) was gradually added, using the ultrasonic bath for both steps (water temperature = 50 °C). AAm and APS were then added following the same procedure described for copolymers. Frontal polymerization was performed: a standard glass test tube (i.e., diameter = 1.5 cm, length = 16 cm) was filled with the polymerization mixture (see above). A thermocouple junction was located at about 1 cm from the bottom of the tube and connected to a digital temperature recorder (Delta Ohm HD 2128.2). The front started by heating the external wall of the tube in correspondence with the upper surface of the monomer mixture until the formation of the front became evident. The polymerization was completed in 18–20 min. Front velocities (V_f) were determined by measuring the front position (easily visible through the glass wall of test tubes) as a function of time. Front temperature (T_{max}) measurements were performed using a K-type thermocouple connected to the digital thermometer (sampling rate: 1 Hz). T_{max} (±10 °C) and V_f (±0.05 cm/min) were measured for all samples. After polymerization, all samples were washed in distilled water at 22 °C for a week to remove DMSO and allow them to swell to equilibrium.

Table 1
Composition and SR% of AAm-GelMA copolymer networks and AAm-GelMA/gelatin semi-IPN hydrogels.

Sample code	GelMA MD	GelMA (wt%)[b]	GelMA methacrylic groups (mol %)[c]	Gelatin (wt%)[d]	AAm/gelatin weight ratio	SR%
Reference sample						
PAAm[a]	–	–	–	–	–	1110
AAm-GelMA copolymer networks						
CAG30-04	30	22.1	0.04	–	–	2870
CAG30-06	30	30.0	0.06	–	–	2460
CAG75-05	75	12.4	0.05	–	–	1460
CAG75-10	75	22.1	0.10	–	–	770
CAG75-14	75	30.0	0.14	–	–	580
Semi-IPN AAm-GelMA/gelatin						
SAG30-20	30	22.1	0.04	3.70	20:1	2600
SAG30-10	30	22.1	0.04	7.20	10:1	2500
SAG30-03	30	22.1	0.04	20.40	3:1	1970
SAG75-20	75	22.1	0.10	3.70	20:1	710
SAG75-10	75	22.1	0.10	7.20	10:1	670
SAG75-03	75	22.1	0.10	20.40	3:1	570

[a] PAAm crosslinked with BIS: 1 mol% of BIS acrylic groups with respect to AAm moles.
[b] Referred to total weight of AAm and GelMA.
[c] Referred to AAm moles.
[d] Referred to the total weight of AAm, GelMA and gelatin.

2.4. Swelling measurements

2.4.1. Swelling ratio and kinetics

All samples were cut into small pieces of similar shapes and sizes and immersed in water to remove DMSO completely. Then, they were dried in an oven at 80 °C and weighed until a constant value to obtain the mass of the dry samples. The swelling kinetics of the hydrogels were determined by immersing the dried hydrogels in water and measuring their weight at gradually increasing time intervals until the weight was constant (swelling equilibrium). The swelling ratio (SR%) was calculated by applying the following equation:

$$SR\% = (M_s - M_d)/M_d \cdot 100 \quad (2)$$

where M_s and M_d are the sample masses in the swollen and dry state, respectively. The graph of SR% as a function of time provides the swelling kinetics of the hydrogel. The reported data are an average of three measurements (reproducibility was about ±10 %). During all the experiments, water temperature was maintained at 22 ± 1 °C.

2.4.2. Swelling/Deswelling cycles

Water-washed hydrogels that reached swelling equilibrium (cycle 0) were subjected to 4 swelling/drying cycles. For each cycle, the value of SR% at the swelling equilibrium and the weight-% of the dry hydrogel, referred to the initial dry weight, were calculated.

2.4.3. Swelling measurements at different temperatures

The swollen hydrogels were subjected to the following temperature ramp: 2, 18, 30, 42, 54, and 70 °C. These values were chosen to investigate the thermal behavior of the hydrogel under different conditions: a temperature close to the freezing point of water (2 °C), room temperature (18 °C), and then temperature intervals of 12 °C up to 70 °C (the last temperature interval was 14 °C). For each temperature, the weight of the hydrogel was measured after 24 h of soaking before moving on to the next temperature. For the measurements at 2 °C, samples were put in a refrigerator, while a thermostatic oil bath was used for temperatures from 30 to 70 °C. After the temperature ramp, the samples that did not dissolve were dried to obtain the M_d value. Considering the experimental error during the measurements, all the SR% values were approximated to the tens.

2.5. Hydrogel characterisations

2.5.1. Thermogravimetric analyses (TGA)

TGA analyses were performed on lyophiliszd samples using a TGA Q500 thermogravimetric analyzer (TA Instruments). The thermograms were recorded from room temperature to 600 °C at a heating rate of 10 °C/min under nitrogen flow

2.5.2. Scanning electron microscopy (SEM)

SEM images were collected using Leica Cambridge Stereoscan 360 and HITACHI 4000 microscopes with an accelerating voltage of 20 kV. Lyophilized samples were immersed in liquid nitrogen for approximately 5 min, cut along their thickness to generate a sample cross-section, and metallized with a gold sputter. The average pore size of samples was determined through radial Power Spectral Density Function (PSDF), denoted as W, measured on SEM images using the software Gwyddion [38]. Böttger et al. [39] reported that the radial PSDF displays few peaks in the semi-logarithmic plot of W vs the reciprocal space $k = \lambda^{-1}$, where λ represents the distance in real space. Each peak signifies the most probable lengths observed in the SEM image. The first peak in the radial PSDF within the k range $\leq 0.03\ \mu m^{-1}$ is excluded due to its strong susceptibility to the inclination and quality of SEM images [40]. Conversely, the second peak has been used to assess the pore diameter Ø. The relative error on Ø was determined by measuring the radial PSDF in three sample regions. Given the significant variability in pore sizes, the relative error is about 30 %. SEM images of lyophilized samples are represented in a grey false color scale with x and y directions calibrated, while the z direction (out of plane, not reported) is in arbitrary units because it is not a topographic height depending on the emission of secondary electrons from the sample. Accordingly, z was used solely to identify pores and the matrix of porous hydrogels, but Ø was evaluated on the image plane, where distances are calibrated.

2.5.3. Rheological analyses

Rheological experiments were conducted using an MCR 102 parallel-plate rheometer (Anton Paar, Graz, Austria) in a plate-plate geometry with a diameter of 25 mm (PP-25 plate) and a gap of 2.0 mm. All samples were precisely cut to obtain cylindrical samples (d = 25 mm, h = 2 mm) and placed on the top of the rheometer plate, following the prior application of silicon oil to prevent the slippage of hydrogels. Subsequently, the upper plate was lowered until contact with the sample's surface. The excess material from the plates was removed with a spatula, and the trap was filled with distilled water to avoid evaporation phenomena.

2.5.4. Amplitude sweep (AS)

Amplitude sweep analyses were performed in a strain range (ɣ) from 0.01 to 1000 % by keeping the frequency constant at 1 rad/s. This test allows the evaluation of the storage modulus (G′) and the loss modulus (G″) as a function of the applied strain (%), the determination of the linear viscoelastic range (LVER), and the crossover point (G′ = G″). All the successive tests were carried out within the LVER.

2.5.5. Frequency sweep (FS)

Frequency sweep analyses were performed in an angular frequency range (ω) from 100 rad/s to 0.1 rad/s by keeping the strain constant at 0.5 %.

2.5.6. Temperature sweep (TS)

The angular frequency and the strain amplitude were kept constant at 0.1 rad/s and 0.5 %, respectively. The starting temperature was set at 4 °C, the final one was set at 60 °C, and a linear ramp of 1 °C/min was applied.

2.5.7. Dynamic strain sweep (DSS)

This test was performed using a controlled shear strain (CSS) mode, and the resulting graph reports G′ and G″ as functions of time. The hydrogel resting condition was simulated by applying a low shear strain (0.1 %). Subsequently, a high shear strain was used, individually determined from the AS test. This determination involved identifying the shear strain value at which the crossover point (G′ = G″) is observed.

2.5.8. Compression tests

Unconfined compression analyses were performed using a universal testing machine (Instron 4465, USA) with a 100 N load cell. Cylindrical samples with a diameter of 10 mm and a height of 10 mm were used for compression tests. Each sample was coated with a thin layer of silicone oil to prevent water loss, and the tests were conducted at a constant compressive rate of 3 mm/min up to the failure point. Compressive modulus (E) was calculated by fitting the initial slope of the stress–strain curves. The compression data are reported as compressive stress versus compressive strain, where compressive stress, σ, was obtained by dividing the force by the original cross-sectional area of the specimen, and the compressive strain, $\varepsilon = \Delta h/h_0$, where Δh is the change in sample thickness, and h_0 is the original sample thickness. The tests were performed in triplicate, following the guidelines of ASTM D695, with appropriate adaptations for hydrogel materials.

2.5.9. Cyclic compression experiment

The cylindrical hydrogel samples were first compressed by a loading cycle to a maximum strain of 30 % with a compression rate of 3 mm/min and then unloaded at the same rate under confined conditions. The area between the loading and the unloading curves estimated the dissipated energy (U_{hys}). The tests were performed in triplicate, following the guidelines of ASTM D695, with appropriate adaptations for hydrogel materials.

3. Results and discussion

This work used the frontal polymerization technique to synthesize both AAm-GelMA copolymer networks and the related semi-IPNs with gelatin as a second network. Fig. 1 shows a scheme of the frontal polymerization of the AAm/GelMA copolymer networks and the semi-IPNs, as well as a sketch of the molecular structure of the resulting materials. Two series of samples were synthesized and characterized to investigate the effect of GelMA and gelatin in acrylamide-based polymer hydrogels. In the first series, AAm-GelMA copolymer networks (CAG series) were prepared, and the effects of both the methacrylation degree (30 or 75 mol%) and its molar amount with respect to the AAm were investigated. The second series (SAG series) of samples consisted of semi-IPN, in which gelatin was added to the AAm-GelMA crosslinked network to study its effect on the CAG hydrogels' properties. In this series, both the GelMA MD (30 or 75 mol%) and the amount of gelatin expressed as the AAm/gelatin ratio were varied. Excluding the reference sample, GelMA also acted as a crosslinker of the AAm in all polymers. Since BIS is one of the most used crosslinkers for acrylamide, it was chosen as the crosslinker in the reference sample.

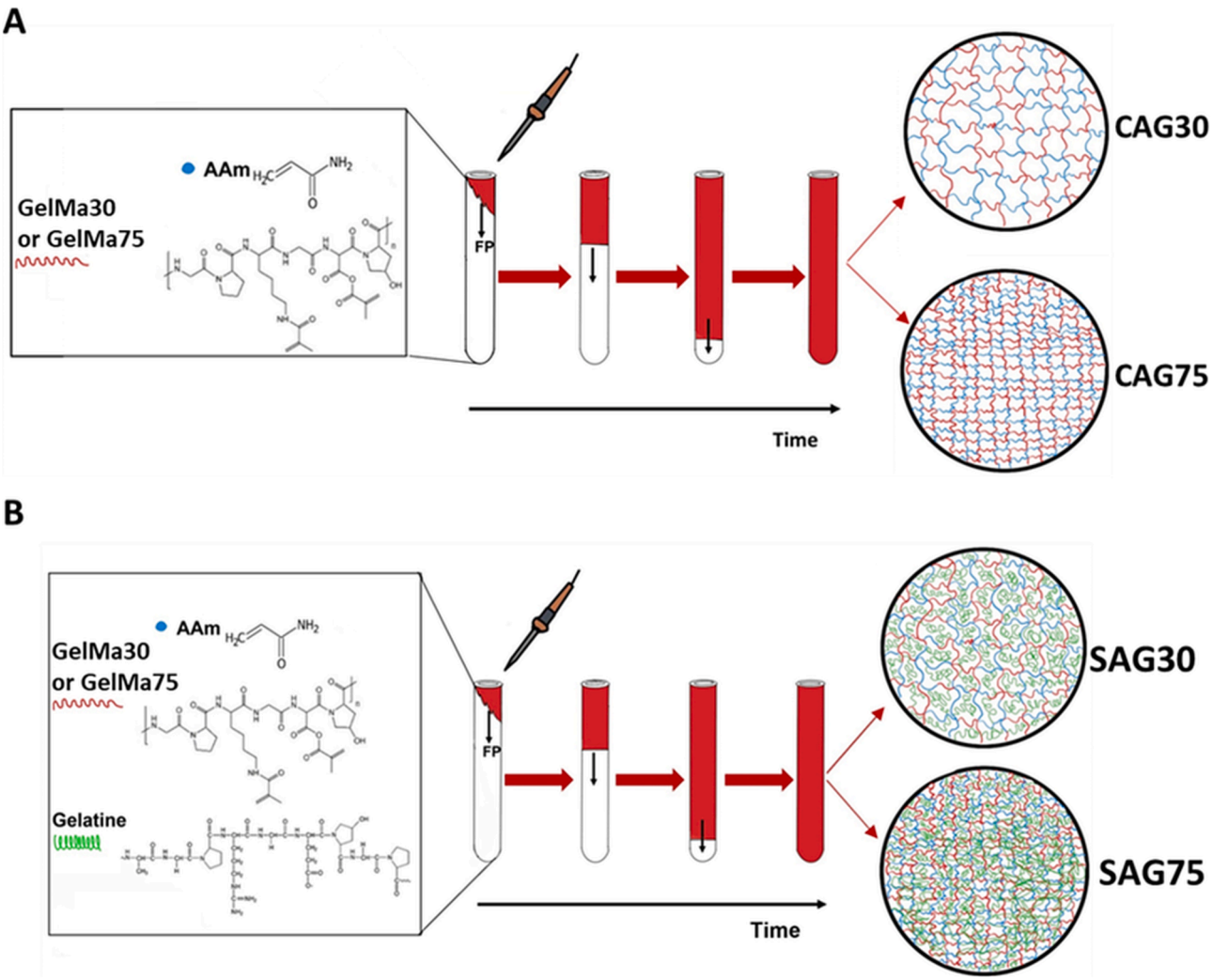

Fig. 1. Scheme of frontal polymerization synthesis of A) AAm-GelMA copolymer networks and B) semi-IPN made of AAm-GelMA copolymer networks and gelatin, and a sketch of the structure of the obtained materials.

Table 1 summarizes the compositions of the hydrogel samples and their respective codes. Preliminary tests were conducted to identify the minimum amount of GelMA suitable to prevent the hydrogel from dissolving. For both series, four different concentrations of GelMA were used: 2.8, 12.4, 22.1, and 30.0 wt% with respect to the total weight of GelMA and AAm. In the series with GelMA30, the threshold value was 22.1 %, corresponding to 0.04 mol% of methacrylic groups with respect to AAm moles. For the samples with GelMA75, this value was 12.4 %, corresponding to 0.05 mol% of methacrylic groups. These results indicate that the higher degree of substitution of methacrylic groups in GelMA75 allowed reaching the minimum crosslinking degree necessary to prevent the hydrogel from solubilization with smaller GelMA weight amounts. We also tried to investigate concentrations of GelMA greater than 30.0 %, but the high viscosity of the system made it difficult to obtain homogeneous and bubble-free solutions. It should also be considered that FP does not allow the quantity of DMSO to be further increased to reduce the viscosity. This causes the front to quench because of excessive heat dissipation.

As regards the composition of the semi-IPNs, we used a GelMA concentration of 22.1 wt% to have a fixed composition of the first network. In contrast, the gelatin concentration (second network) was allowed to vary, as reported in Table 1. The upper concentration limit of the gelatin was determined by the achievement of too high viscosities of the polymerization mixture.

Also, a preliminary study was conducted for the reference sample to determine the concentration of BIS necessary to obtain a hydrogel crosslinked enough that it does not dissolve. Complete solubilization of the hydrogel was observed using an acrylic group molar concentration equal to that used for the samples with GelMA (0.10 mol%). It has been found that, with the classic BIS crosslinker (with the concentrations of initiator and solvent used in this work), the amount necessary to obtain a compact hydrogel is 1 mol%. This result indicates that crosslinking with GelMA is much more effective than crosslinking with BIS since the concentration of methacrylic groups necessary to obtain a compact hydrogel is an order of magnitude lower. This is due to the interactions between the GelMA chains, which give rise to further physical crosslinking that adds to the chemical one.

Regarding FP runs, it was observed that a constant front velocity (here, not shown) was obtained for all samples, and pure FP occurred (i.e., no side reactions co-occurred). The composition of the hydrogels influences the FP parameters in a limited manner (see Supplementary Information, Table S1). It was observed that for all samples, T_{max} remained constant around an average value of 100 ± 10 °C. Front velocity was slightly influenced by the methacrylation degree of GelMA. In the samples with GelMA75, V_f remains constant at 0.45 ± 0.10 cm/min, while in the samples with GelMA30, it varies from 0.45 to 0.25 ± 0.10 cm/min as the concentration of GelMA increases. This difference can be attributed to the greater reactivity and less heat dissipated in GelMA75. To our knowledge, this is the first published work in which FP is exploited to copolymerize GelMA. It should also be highlighted that

gelatin does not cause any variations in the FP parameters.

Fig. 2 shows the swelling kinetics of the two series of samples. The trend of SR% as a function of time is very similar for all samples: initially, a rapid increase in SR% as a function of immersion time in water is observed; after ca. 2000 min, the weight begins to stabilize until it reaches a plateau, in which the hydrogel has achieved swelling equilibrium in water. The only exception to this behavior is observed in the SAG30-20 sample in which, after 570 min, there is an abrupt change in the slope of the curve due to partial dissolution of the hydrogel. The equilibrium swelling values are reported in the last column of Table 1, and they can be correlated to the composition of the various samples. As regards the copolymers, the SR% decreases by increasing the GelMA amount, and there is a marked difference between the samples with GelMA30 and those with GelMA75. The former swells much more due to the lower crosslinking density, and the SR% values (>2400 %) are also significantly higher than the PAAm reference (1110 %). Copolymers with GelMA75 have much lower swelling values; for CAG75-10 and CAG75-14 samples, SR% (values = 770 and 580 %, respectively) is lower than the value of polyacrylamide crosslinked with BIS (PAAm). This is because the quantity of methacrylic groups (0.10 and 0.14 mol%) is higher than that of GelMA30 (0.04 and 0.06 mol%, see column 4 of Table 1). It is essential to highlight that the reference PAAm contains an amount of crosslinker (1 mol%) which is two orders of magnitude higher than the samples with less GelMA (0.04 or 0.05 mol%): thus, crosslinking with GelMA is much more effective, and this can be explained by taking into account the GelMA-GelMA physical interactions. By considering the samples containing gelatin (semi-IPN series), it is possible to observe a decrease in the swelling ratio as the concentration of gelatin increases for both SAG30 and SAG75 samples. In this case, it must be taken into account that gelatin is dispersed within another polymer network (PAAm-GelMA): the rearrangement of the chains for the formation of the secondary structure typical of gelatin is hindered because of the lower freedom of movement of the polypeptide chains. On the other hand, one must also consider the interactions established between gelatin and GelMA, which justify an increase in physical crosslinking as the concentration of gelatin increases, with a consequent decrease in SR% values.

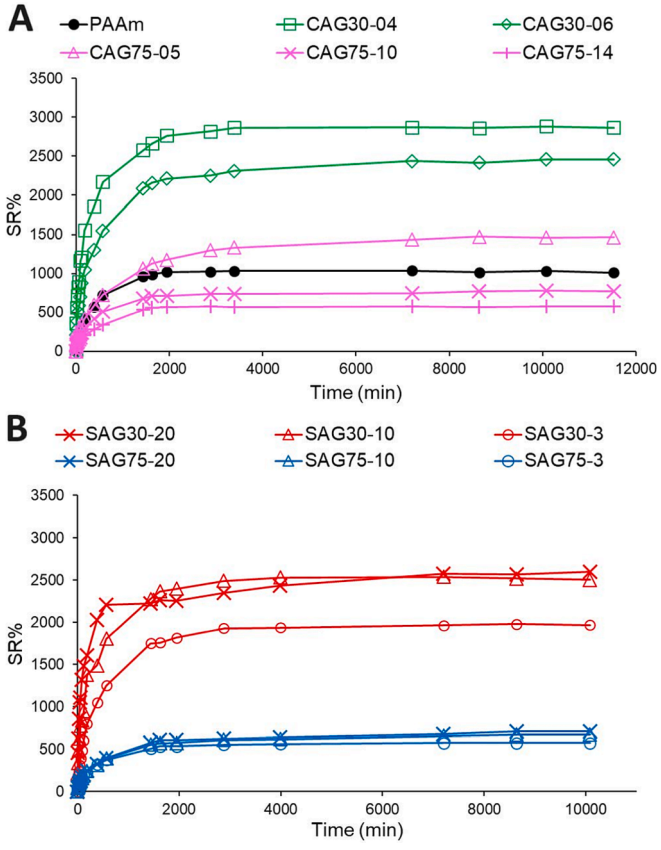

Fig. 2. Swelling kinetics of (A) AAm-GelMA copolymer networks and (B) AAm-GelMA/gelatin semi-IPN hydrogels.

To verify both the ability to maintain the swelling capacity and check the possible partial solubilization of the hydrogels in water, they were subjected to four swelling/drying cycles. Fig. 3 reports both the SR% values and the dry weight in the four cycles for the two series of samples: (A) copolymers, and (B) semi-IPN. For the CAG series, it was observed that both the reference and the CAG30 samples undergo a reduction of SR% and dry weight from cycle to cycle. For reference, the SR% and the dry weight loss vary, especially in the first cycle, in which the dissolution of unreacted monomer, or BIS, occurs. In samples with GelMA30, SR% and dry weight loss continue to vary in each cycle. This result could be due to the low crosslinking density, which over time leads to the dissolution of GelMA fractions initially bound to the polymer only by physical interactions. In the CAG75 samples, no significant variations in SR% are observed, and the dry weight losses are negligible: the greater crosslinking density of the hydrogel allows it to retain the low molecular weight fraction that would otherwise dissolve in water.

As regards the SAG series, the difference in the behavior of samples containing GelMA30 and GelMA75 was confirmed. For the SAG75 samples, no appreciable differences in SR% and dry weight loss were observed as a function of the gelatin concentration. On the contrary, in samples with GelMA30, the effect of gelatin concentration can be evaluated. By increasing the amount of gelatin, the crosslinking density increases, and the partial solubilization of the low molecular weight components is hindered. Further studies on the solubilized fraction and the correlation between dry weight loss and a decrease in SR% will be performed.

Since gelatin in water presents a characteristic sol–gel transition when cooled (T_{trans} = 26–30 °C), the variation of SR% as a function of temperature was also studied. Table 2 shows the trend of SR% as a function of temperature for the CAG and SAG series. It can be observed that the copolymers with GelMA30 completely dissolve between 30 and 42 °C; on the other hand, for copolymers with GelMA75, no solubilization is observed. In other words, the increase in temperature causes an increase in SR%, and it can also be pointed out that it is inversely proportional to the degree of crosslinking. These trends can be explained by considering that the chemical crosslinking in the samples with GelMA30 is very mild, and the hydrogel remains compact because of the physical crosslinking caused by GelMA. Increasing the temperature, these interactions weaken, and the hydrogels dissolve entirely between 30 and 42 °C. In hydrogels with GelMA75, the greater degree of chemical crosslinking prevents the dissolution of the hydrogels. As the temperature increased from 2 to 70 °C, the physical interactions responsible for the physical crosslinking were reduced, and a consequent increase in SR % was observed. In the passage between 54 and 72 °C, a very high rise in SR% was observed, especially for the CAG75-20 and CAG75-10 samples. It could be hypothesized that in this interval, GelMA75 reaches a switching temperature at which the physical interactions among the chains are thermodynamically unfavored compared to GelMA-water interactions. As regards the reference, no trend of the swelling ratio as a function of temperature was observed, and the SR% values fluctuate around 1700 %.

For the semi-IPN series, the solubilization of the samples crosslinked with GelMA30 was confirmed even in the presence of gelatin. For the samples with GelMA75, in the temperature range from 2 to 54 °C, there was no significant variation in the SR% values as the gelatin concentration increased. Conversely, going from 54 to 70 °C (switch temperature, see above), an increase in the degree of swelling was observed, and it was inversely proportional to the concentration of gelatin in the semi-IPN.

Finally, it was noticed that when the hydrogels were brought back to

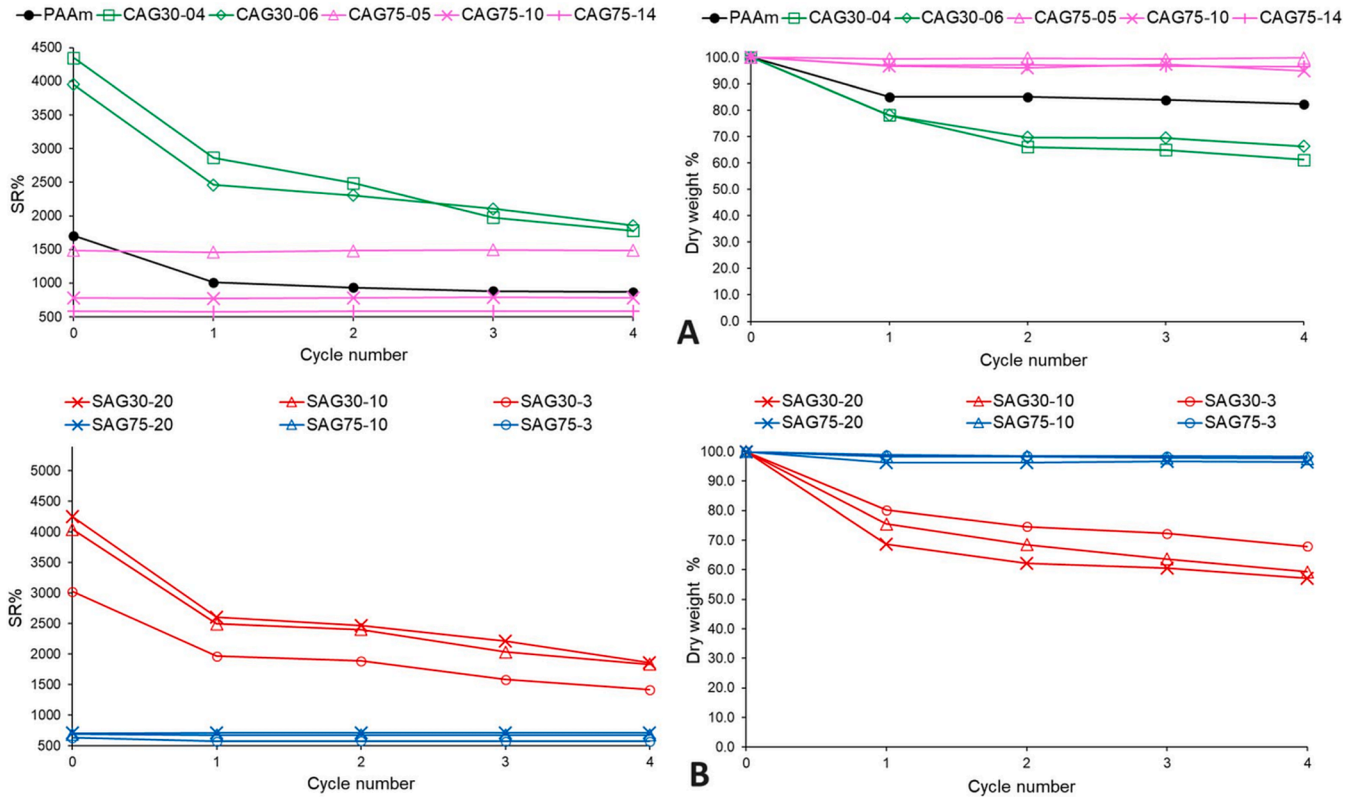

Fig. 3. Swelling ratio and dry weight loss as a function of swelling/drying cycle number for the (A) AAm-GelMA copolymer networks and (B) AAm-GelMA/gelatin semi-IPN hydrogels.

Table 2
Swelling ratio as a function of temperature for the AAm-GelMA copolymer networks and AAm-GelMA/gelatin semi-IPN hydrogels.

T (°C)	SR% of copolymer networks					
	PAAm	**CAG30-04**	**CAG30-06**	**CAG75-05**	**CAG75-10**	**CAG75-14**
2	1600	3750	3660	1390	780	580
18	1760	3890	3770	1450	840	630
30	1690	d[a]	5220	1570	890	640
42	1710	d	d	1680	900	650
54	1580	d	d	1890	960	660
70	1830	d	d	6650	1770	810

T (°C)	**SR% semi-IPN**					
	SAG30-20	**SAG30-10**	**SAG30-03**	**SAG75-20**	**SAG75-10**	**SAG75-03**
2	3780	3690	2190	720	630	670
18	3900	3860	2930	760	670	700
30	d[a]	5350	4690	810	710	720
42	d	d	d	830	730	730
54	d	d	d	870	750	740
70	d	d	d	1380	1210	810

[a] d = dissolved.

room temperature, they did not undergo a decrease in SR%: the physical interactions between the GelMA and gelatin chains did not reform due to the limited freedom of movement.

Thermogravimetric analysis was carried out to confirm the presence of the different components in the obtained copolymers and semi-IPNs. The degradation temperature (T_{degr}) and weight loss (%) of the various samples are reported in Table S2. To clearly visualize the different degradation steps, Fig. 4 shows the derivative of the weight loss (%) of the analyzed samples with respect to temperature. Fig. 4(A) compares PAAm, GelMA30, and their copolymer CAG30-04: PAAm degradation occurs in two pyrolysis stages, while GelMA30 degradation occurs in one step with T_{degr} equal to 330 °C. The CAG30-04 curve confirms the trend followed by PAAm, with the appearance of a hump in between the two peaks at 297 °C and 390 °C, which is related to the presence of GelMA30 within the formed network. Fig. 4(B) compares the series with PAAm, GelMA75, and CAG75-10. Also in this case, the presence of GelMA is confirmed in the CAG75-10 by the hump between 293 °C and 405 °C. In the SAG series, gelatin was incorporated into the network to obtain the semi-IPN samples. Therefore, a comparison between gelatin, the starting copolymer (CAG30-04 and CAG75-10), and the SAG samples was carried out (Fig. 4(C, D)). For the series including GelMA30 (Fig. 4(C)), it is observed that the hump characterizing CAG30-04 between 297 °C and 390 °C is more pronounced as the gelatin content increases, and it is also overlapping with the gelatin peak at 319 °C. Concerning the series with GelMA75 (Fig. 4(D)), a slight increase of the peak at 350 °C is visible, increasing in intensity with increasing amounts of gelatin. These results allowed us to qualitatively confirm the presence of the different components of synthesized samples, and assess their degradation temperatures.

Regarding morphological analysis, visual inspection of SEM images was performed along with their analysis using radial average Power Spectral Density (PSD). This analysis enabled the visualization of the role of composition on the overall morphology. The reference samples PAAm, GelMA30, and GelMA75 are reported in Fig. 5(A), 5(B), and 5 (H), respectively, along with their combinations for producing AAm-GelMA copolymer networks (first and third rows of Fig. 5). CAG30-04 in Fig. 5(C) is made by combining PAAm and GelMA30, while CAG75-10 in Fig. 5(I) is produced by combining PAAm and GelMA75. SAG30 and SAG75 series in Fig. 5(D-F) and 5(J-L) show the gelatin effect on CAG30-04 and CAG75-10, respectively. All hydrogels can be defined as porous materials [41], as they contain pores of varied sizes in a skeletal

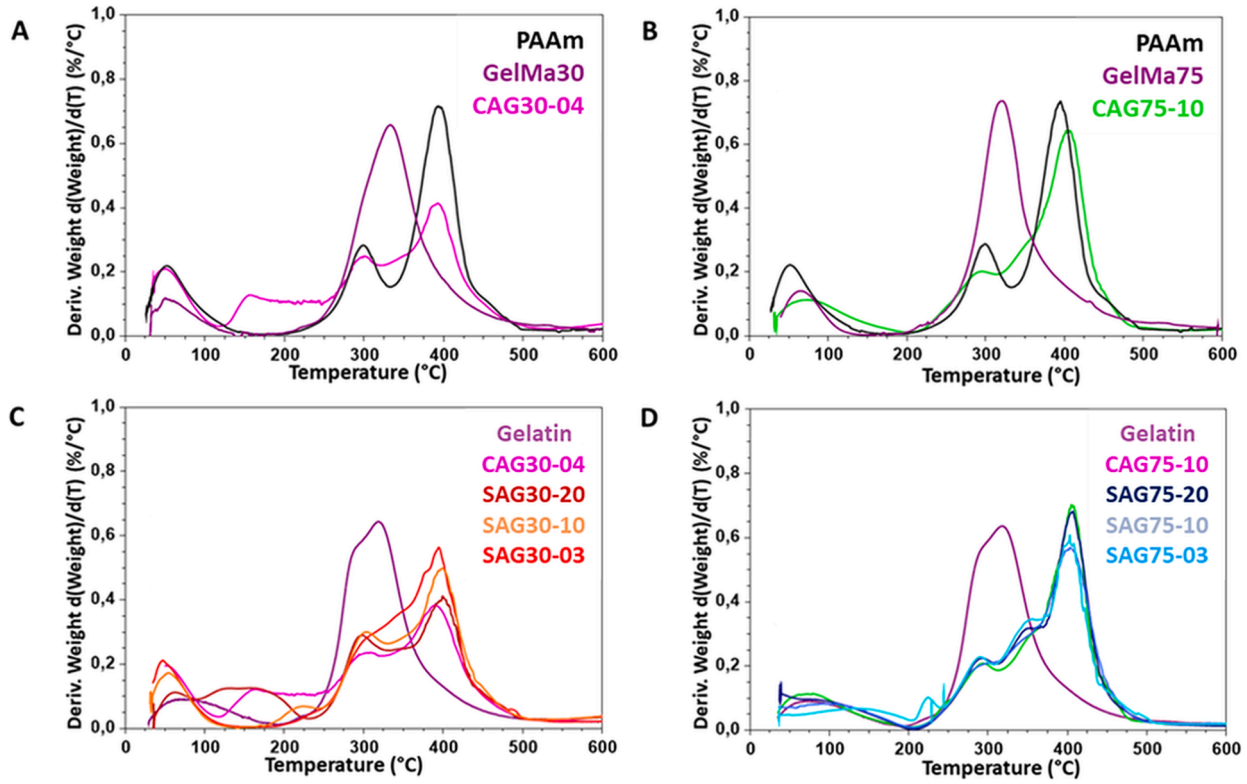

Fig. 4. Results of thermogravimetric analysis (TGA) on lyophilized AAm-GelMA copolymer networks, AAm-GelMA/gelatin semi-IPN hydrogel samples and reference polymers PAAm, Gelatin and GelMA.

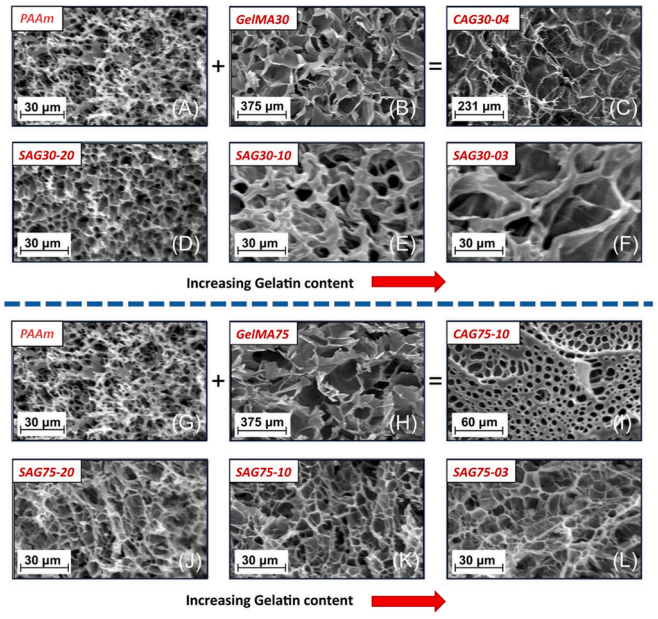

Fig. 5. SEM images of hydrogel samples: reference sample, AAm-GelMA copolymer networks (A-C and G-I) and morphological effects on them due to the increase of gelatin content (D-F and J-L). Image magnifications and correspondent scale bars of AAm-GelMA copolymer networks without gelatin (A-C and G-I) are different to show the matrix structure of pores at largely different length-scale. On the other hand, SEM images of morphological effects due to gelatin (D-F and J-L) have the same scale bar.

matrix with variable width.

AAm-GelMA copolymer networks show opposite morphologies; CAG30-04 has large pores with Ø = 23 ± 7 μm, in line with those of GelMA30, i.e., Ø = 21 ± 6 μm, while CAG75-10 is characterized by smaller pores, Ø = 1.7 ± 0.5 μm, similar to those of PAAm, Ø = 1.4 ± 0.4 μm. In this latter case, smaller pores are accompanied by a thickened matrix (see Fig. 5(I)). These different characteristics of the two types of copolymers also explain the much larger SR% values obtained for the copolymers with GelMA30 compared to the copolymers with GelMA75 (see Table 1).

The effect of gelatin on CAG30-04 is remarkable: the large pores observed in Fig. 5(C) are reduced to Ø = 1.8 ± 0.5 μm (see Fig. 5(D)) even for the lower concentration of gelatin and, concurrently, the matrix is thickened. Progressively increasing gelatin concentration, pores increase (Ø ≈ 1.8, ≈ 2.2, and ≈ 2.9 μm for SAG30-20, SAG30-10, and SAG30-03, Fig. 5(D-F)). Such an increase is evident in SEM images, although experimental errors on pore sizes make them comparable (Ø = 1.8 ± 0.5, 2.2 ± 0.7 and 2.9 ± 0.9 μm for SAG30-20, SAG30-10 and SAG30-03, respectively). On the other hand, gelatin on CAG75-10 preserves pores sizes (Ø = 1.9 ± 0.6 μm for SAG75-20, see Fig. 5(J)) but thins the matrix. By progressively increasing gelatin concentration, the structure of hydrogels does not change (Ø = 2.0 ± 0.6 and 2.1 ± 0.6 μm for SAG75-10 and SAG75-03, respectively – Fig. 5(K, L)).

As regards rheological properties, oscillatory analyses were performed to determine how the stiffness and rigidity of materials vary according to the different amounts of components and to assess how the presence of gelatin in the network, namely the passage from copolymers to semi-IPN networks, affects the properties of the final material. Amplitude sweep tests allowed the determination of G′ and G″ moduli and crossover point (Table S3). Fig. 6(A) and 6(B), respectively, report the G′ and G″ moduli curves of PAAm, CAG30-04, and SAG30 series samples. It can be noticed that CAG30-04 shows a trend like the starting PAAm sample, but it shows a crossover point, meaning that an increase in rigidity is obtained when the copolymer network is formed. At the same time, when gelatin is intercalated within this network, forming the semi-IPN, a substantial decrease in the moduli is registered. These considerations are valid for SAG30-20 and SAG30-10, with no

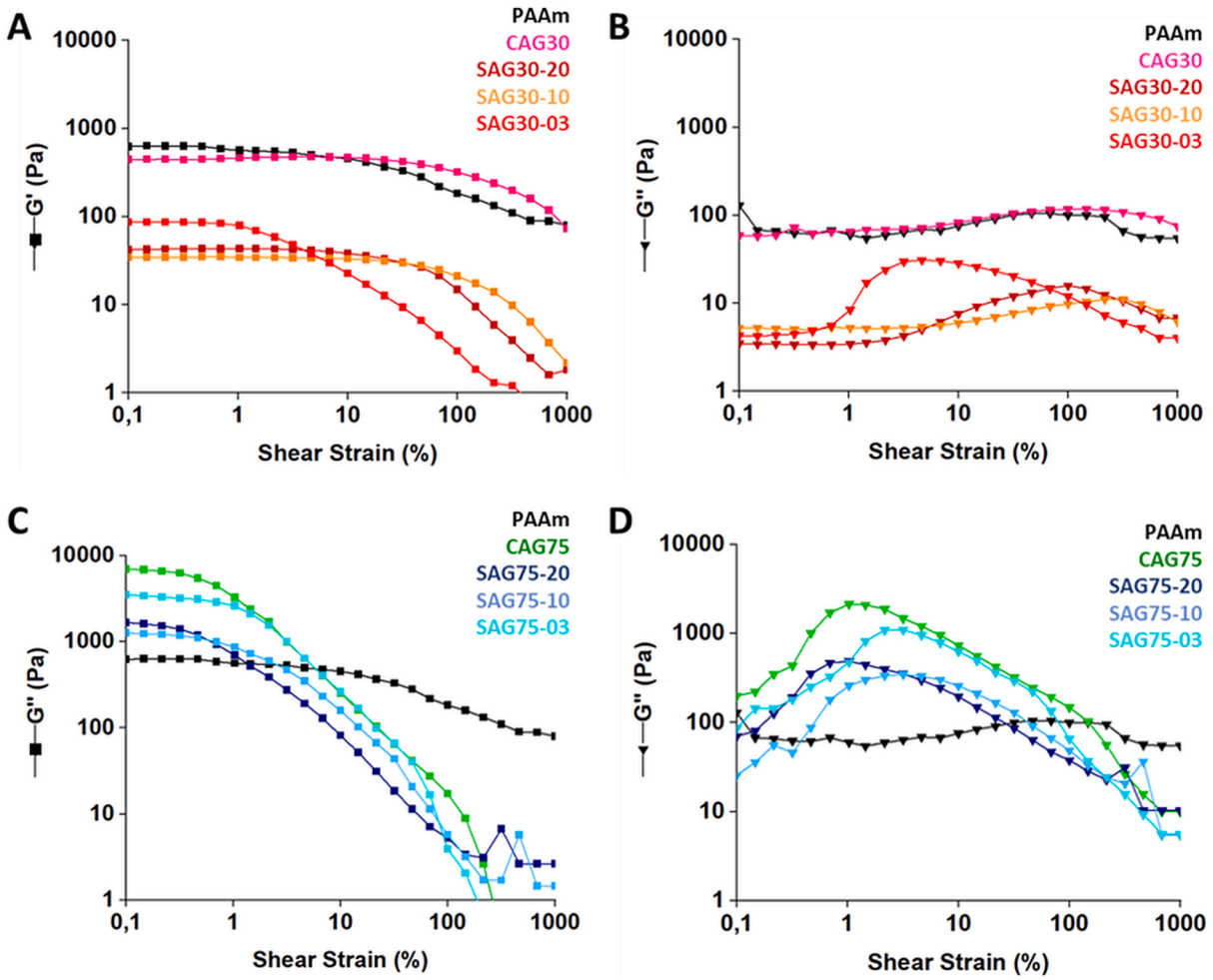

Fig. 6. Amplitude Sweep experiments of hydrogel samples. (A, C) Storage moduli, G′, and (B, D) loss moduli, G″, as a function of the applied shear strain for reference sample, AAm-GelMA copolymer networks, AAm-GelMA/gelatin semi-IPN with GelMA30 and GelMA75, respectively.

significant difference between the samples. The self-aggregation of gelatin macromolecules results in a softer gel for SAG30-20 and SAG30-10. A different behavior is observed for the SAG30-03 sample: it is the most rigid sample of the series, with a crossover point occurring at 10 % shear strain. This means that, beyond a specific concentration, excess gelatin not only undergoes self-aggregation of macromolecular chains but also establishes physical interactions with the copolymer network, contributing to an increase in its rigidity. Fig. 6(C, D) reports the same tests applied to the series of samples with GelMA75. Comparing the G′ and G″ curves of PAAm and CAG75-10, a substantial increase in the rigidity occurs with the formation of the copolymer due to the higher MD of GelMA. Then, with the introduction of gelatin to form the semi-IPN, a decrease in the moduli with respect to the starting copolymer CAG75-10 is noticed. Also in this case, no significant difference between SAG75-20 and SAG75-10 is present, while for the SAG75-03 sample, which contains a higher amount of gelatin, an increase in the moduli is obtained. This is again ascribed to the physical crosslinking among gelatin chains coming into play when gelatin content increases, forming a more interlocked and rigid network. Generally, when the materials are prepared starting from the less substituted GelMA30, soft and elastic samples are obtained, while more rigid and stiff materials characterize the GelMA75 sample series. The different methacrylation degrees of GelMA and the different gelatin content employed for the semi-IPNs preparation can be exploited to tune the final properties of the materials according to the various targeted applications.

The frequency sweep is the second oscillatory test performed to gain insights into the microstructure of the obtained materials. As shown in Figure S1, all hydrogel samples exhibited an elastic response, with the G′ modulus exceeding the G″ modulus values over the whole frequency range, indicating that the chain motions in the hydrogel network were restricted and the materials were kept at a stable gel-like state. Again, samples prepared starting from GelMA75 displayed higher moduli than those with GelMA30 due to the higher crosslinking density.

The thermal stability of the samples was investigated through temperature sweep tests from 5 to 60 °C (Fig. 7(A, B, C)). For greater clarity, only the graphs of some samples are shown. Other graphs are reported in Supplementary Information (Fig. S2(A)). All samples showed G′ values higher than G″ ones in the whole temperature range, indicating that strong crosslinked structures were obtained. PAAm and high crosslinked copolymer CAG75-10 (Fig. 7(A)) samples do not show any temperature dependence. Regarding CAG30-04, moduli decrease is observed at 34 °C, resulting in a weaker gel network. The same trend is observed for the semi-IPN samples, suggesting that SAG75-20, SAG75-10 and SAG75-03 can be employed in higher temperature applications without losing their mechanical integrity. SAG30 hydrogels exhibited temperature-dependent behavior, with a noticeable decrease in G′ and G″ moduli observed at temperatures higher than 36 °C (refer to Table S4), resulting in weaker gel networks. This behavior, therefore, confirms the results obtained with the swelling tests performed at different temperatures (see Table 2). As stated above, this could be attributed to the less densely connected network observed in SAG30 samples compared to SAG75 samples. Therefore, thermosensitive gelatin cannot be physically entrapped within the less dense network, resulting in a coil-helix transition as temperature increases [34].

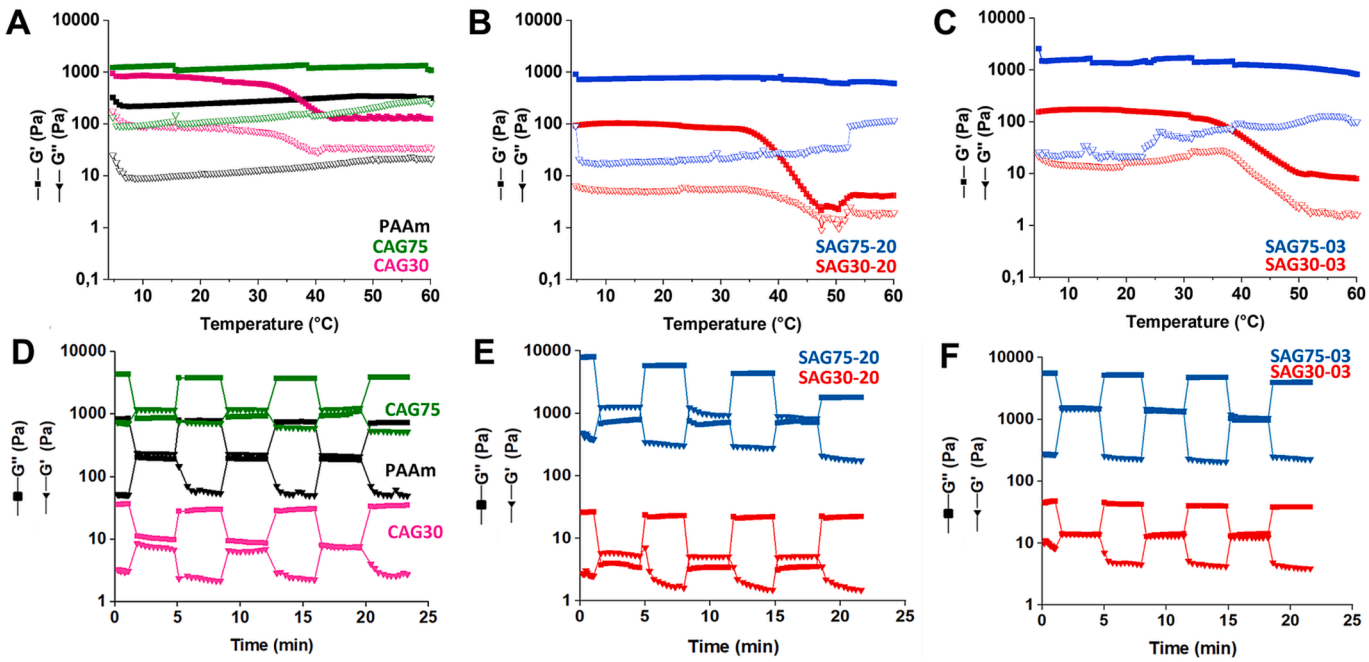

Fig. 7. Temperature sweep experiments. G′ and G″ as function of temperature for (A) PAAm and AAm-GelMA copolymer networks and (B, C) for AAm-GelMA/gelatin semi-IPN. *Dynamic strain sweep experiments*. G′ and G″ as a function of the time applying a cyclic low–high strain sweep for (D) PAAm and AAm-GelMA copolymer networks and (E, F) for AAm-GelMA/gelatin semi-IPN.

Finally, the dynamic shear strain test was employed to evaluate the mechanical recovery properties of reference samples, copolymers, and semi-IPNs. Again, not all samples are reported here for better clarity, but more graphs can be found in Supporting Information (Fig. S2(B)). This assessment is crucial since the macroscopic change in G′ and G″ values can signify the rupture and repair of the hydrogel microstructure. The previously reported amplitude sweep test determined the linear viscoelastic region of hydrogels (Fig. 6). The crossover point, corresponding to the intersection of G′ and G″, was established at approximately 300 % for PAAm, CAG30-04, and SAG30 hydrogels. In contrast, for CAG75-10 and SAG75 hydrogels, characterized by a more rigid and brittle mechanical behavior, the crossover point was approximately 10 %. After these shear strain (%) values, G″ becomes equal to or higher than G′, indicating the rupture of the hydrogel internal microstructure. As shown in Fig. 7(D, E, F), hydrogels were subjected to alternately low (0.1 %) and high (300 % or 10 %) shear strain, revealing a transition from a gel state ($G' > G''$) to a liquid-like state ($G'' > G'$) as the shear strain increased, signifying damage to the internal structure. However, after the shear strain returned to 0.1 %, G′ and G″ values promptly returned to the original values, underscoring the exceptional recovery ability of the samples. The hydrogels demonstrated an impressive capability to rapidly rebuild the internal network when the shear strain was lowered back to 0.1 %. Physical interactions (e.g., hydrogen bonds) within the hydrogel network broke under external forces, leading to network destruction, but upon cessation of external forces, reversible physical interactions were re-established. Consequently, the hydrogel effectively dissipates energy through the rupture of sacrificial bonds, resulting in excellent recovery capability and reliable mechanical properties.

Fig. 8(A) shows that hydrogels can be compressed several times and recovered. Compression tests were performed to investigate quantitatively the developed hydrogels' mechanical properties. Young's modulus can represent the strength of the gel, while the elongation reflects its deformability. Fig. 8(B) shows the stress–strain curves of PAAm, CAG30-04, and CAG75-10 under uniaxial compression. Starting from the copolymers, the type of GelMA influenced the compression properties: CAG30-04 showed a better elongation at break (155 %) than CAG75-10 (117 %) since it is less crosslinked. However, due to the less dense crosslinked network, CAG30-04 resulted in a weaker hydrogel (Young's modulus at 30 % of 0.006 kPa) than CAG75-10 (Young's modulus at 30 % of 0.02 kPa). Moving to the semi-IPNs, it is easy to observe that the introduction of gelatin profoundly influences compression values.

As shown in Fig. 8(C, D), by increasing the gelatin concentration, a slight increase of compression moduli in the SAG30 series and a slight decrease of compression moduli in the SAG75 series are observed (Table S5). The determining parameter of the mechanical properties is GelMA MD: the SAG30 series showed fracture stress values lower than those of the SAG75 one, with the same gelatin content. Indeed, as the degree of intermolecular crosslinking increased, the density of the network structures increased, too, thus enhancing the required force to destroy the hydrogels' structure.

Passing from CAG30-04 to SAG30 samples, strain values at rupture decreased. Regarding samples with GelMA75, the elongation at break of the SAG75 series was higher than CAG75, indicating a synergistic effect between the secondary network of gelatin and the first copolymer network, which optimizes the performance of the gels. However, as the gelatin content increased, the elongation at break decreased, indicating that the higher degree of crosslinking negatively affected the elongation at break.

To elucidate the energy dissipation mechanism of hydrogels, crucial for practical applications, samples underwent four consecutive loading–unloading compression tests at a constant strain of 30 % and a rate of 3 mm/min. The energy dissipation capability of the hydrogel was observed to increase with an increase in the hysteresis loop. As illustrated in Fig. 8(H), the stress–strain curves reveal that PAAm hydrogel exhibits an energy dissipation of 1502 J/m^3, with the hysteresis loop nearly overlapping for the subsequent three cycles, indicating robust self-recovery. Regarding the copolymers, the incorporation of GelMA significantly enhances toughness. In the initial compression cycle, CAG30-04 displays a dissipation energy of 2687 J/m^3, maintaining a consistent hysteresis loop until the fourth cycle (887 J/m^3). In contrast, CAG75-10 demonstrates higher dissipation energy (4521 J/m^3), with a slight decrease in subsequent cycles (3580 J/m^3). In the first loading–unloading cycle, chemical crosslinking and hydrogen bonds

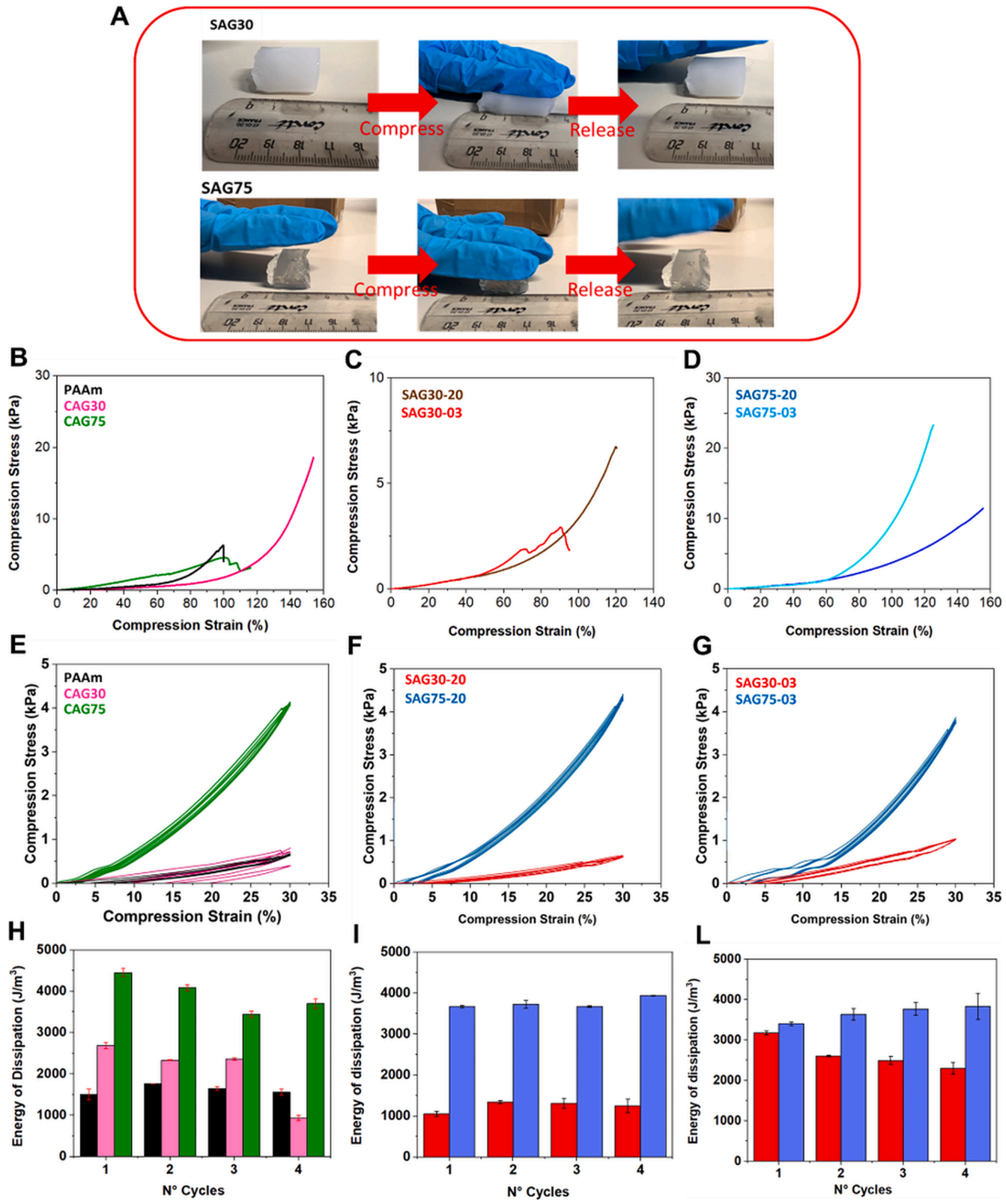

Fig. 8. (A) SAG30 and SAG75 hydrogels could withstand compression and maintain their shape. Compression stress–strain tests for (B) reference samples and AAm-GelMA copolymer networks, (C) SAG30 series, and (D) for SAG75 series; recovery cyclic compression stress–strain tests, without intervals for (E) reference sample and AAm-GelMA copolymer networks, and for (F, G) AAm-GelMA/gelatin semi-IPN; energy of dissipation of (H) PAAm (black), CAG30-10 (pink), CAG75-04 (green); (I) SAG30-20 (red), SAG75-20 (blue); (L) SAG30-03 (red), SAG75-03 (blue).

undergo partial rupture, inducing an extensive hysteresis loop. Due to the permanent collapse of chemical crosslinking, the second cycle exhibited a smaller hysteresis loop. Subsequently, the hysteresis loops were almost overlapped for the following three cycles, indicating that the hydrogels have favorable fatigue resistance and self-recovery. Moreover, an increase of the hysteresis loop from CAG30-04 to CAG75-10 may be attributed to the better capability to dissipate energy of the homogenous structure of the CAG75-10, where network damage could be recovered through the alignment of polymer chains and restoration of hydrogen bonds after disruption. Moving to the SAG30 series, it is easy to observe that the hysteresis loops were almost overlapped for the cycles, indicating that the hydrogels have favorable fatigue resistance and self-recovery. Conversely, the SAG75 series exhibits enhanced dissipated energy, attributable to the synergistic effect between the secondary network of gelatin and the primary copolymer network, optimizing the toughness of the gels. Moreover, the dissipated energy increases by increasing the number of hysteresis loops.

4. Conclusion

In this work, PAAm-based hydrogels containing GelMA were synthesized for the first time by frontal polymerization. GelMA with two different degrees of methacrylation (30 and 75 mol%) was exploited to obtain both copolymers with acrylamide (GelMA acted as a crosslinker) and semi-IPNs with a second gelatin network. As a first significant result, we found that PAAm crosslinking by GelMA is much more effective than by using BIS, since the concentration of methacrylic groups necessary to obtain a compact hydrogel is two orders of magnitude lower with GelMA (0.04 mol%) than with BIS (1 mol%). This is due to the interactions between GelMA chains, which give rise to further physical crosslinking (i.e., GelMA-GelMA interactions) additional to the chemical crosslinking (due to methacrylic groups), leading to improved mechanical properties.

Concerning copolymers, the degree of substitution of GelMA represented a critical parameter that significantly influenced the properties of the final hydrogels. In copolymers containing GelMA75, the high amount of methacrylic groups resulted in a polymer with a high degree of crosslinking, in which the pore size of the hydrogel was small (≈1.7 μm) and the SR% (average value ≈ 940) was low as compared to that of BIS-crosslinked polyacrylamide (1110). Conversely, using GelMA30, copolymers with a low degree of crosslinking were obtained, and a larger pore size (≈ 23 μm) and a high SR% value (up to 2900) were found. This also led to the complete dissolution of the hydrogels at temperatures above 34 °C, at which the coil-to-helix transition of gelatin and the consequent decrease in physical interactions resulted in the complete dissolution of the hydrogels. On the other hand, CAG75 copolymers were stable: the high crosslinking density allowed the soluble fractions to be retained in successive swelling/drying cycles and at elevated temperatures (up to 70 °C). Temperature sweep tests also confirmed stability at elevated temperatures. Finally, rheological and compression tests showed that when the materials were prepared starting from the less substituted GelMA30, soft and elastic samples were obtained (E_{t30} compression modulus = 0.006 KPa for CAG30-04 sample), while the GelMA75 series was characterised by more rigid and stiff resulting materials (E_{t30} compression modulus = 0.02 KPa for CAG75-10 sample). GelMA MD in copolymers with acrylamide allowed the tuning the properties of the hydrogels: swelling capacity, mechanical and rheological properties, solubility, and resistance to elevated temperatures can be modulated by appropriately varying the quantity of methacrylic groups present in the GelMA comonomer.

The other fundamental objective of the work was to study the effect of adding gelatin (second network) to the AAm-GelMA copolymer networks to obtain a semi-IPN (SAG series). In these samples, gelatin chains interacted with each other and with GelMA chains through the formation of hydrogen bonds, like what happened in gelatin hydrogels. The formation of these hydrogen bonds, which led to further physical crosslinking, was confirmed by TGA analyses, which showed an increase in the degradation temperature of gelatin in the semi-IPN. This physical crosslinking effect was particularly evident in the hydrogels' rheological and mechanical properties. Rheological tests showed that when low amounts of gelatin were intercalated within the CAG network (AAm/gelatin weight ratio higher than 10:1), a substantial decrease of the moduli (i.e., G′ moved from 446 to 34 Pa for the hydrogels with GelMA 30, and from 6820 to 1232 for the hydrogels with GelMA 75) and increased elasticity were observed due to the interference with the copolymer network and self-aggregation of gelatin chains. For higher amounts of gelatin (AAm/gelatin weight ratio 3:1), the physical interactions with the copolymer network significantly increased, thus resulting in the formation of a more interlocked and rigid network, causing an increase in hydrogel modulus and stiffness (i.e., G′ moved from 34 to 86 Pa for the hydrogels with GelMA 30, and from 1232 to 3412 Pa for the hydrogels with GelMA 75). Moreover, dynamic shear strain tests proved that all hydrogels possessed exceptional recovery ability. Indeed, they had a high capability to rebuild the internal network rapidly when the shear strain returned to low values. When hydrogels were subjected to high shear stress, physical interactions (e.g., hydrogen bonds) within the hydrogel network were broken, leading to network destruction. However, upon cessation of external forces, reversible physical interactions were re-established. Consequently, the hydrogel effectively dissipated energy through the rupture of sacrificial bonds, resulting in excellent recovery capability and reliable mechanical properties.

Overall, our study has unveiled a versatile platform for tailoring hydrogel properties through gelatine and GelMA incorporation: according to the different degrees of substitution of GelMA and various amounts of incorporated gelatine, it is possible to tune the resulting porosity, mechanical properties, and swelling behaviour, making these systems suitable for a wide range of applications in materials and biomedical fields.

5. Funding sources

The PhD scholarship of LDL was funded by the European Union – NextGenerationEU through the Italian Ministry of University and Research under PNRR – Mission 4 Component 2, Investment 3.3 "Partnerships extended to universities, research centers, companies, and funding of basic research projects" D.M. 352/2021 – CUP J33C22001330009.

This work was partially financed by the University of Sassari (FAR 2023, and 2024 funds).

CRediT authorship contribution statement

Luana Di Lisa: Writing – original draft, Visualization, Investigation, Conceptualization. **Mariangela Rea:** Writing – original draft, Visualization, Investigation, Conceptualization. **Daniele Nuvoli:** Writing – review & editing, Writing – original draft, Supervision, Conceptualization. **Maria Letizia Focarete:** Writing – review & editing, Supervision, Conceptualization. **Cristiano Albonetti:** Visualization, Investigation, Formal analysis. **Alberto Mariani:** Writing – review & editing, Supervision, Conceptualization.

Declaration of competing interest

The authors declare that they have no known competing financial interests or personal relationships that could have appeared to influence the work reported in this paper.

Appendix A. Supplementary data

Supplementary data to this article can be found online at https://doi.org/10.1016/j.eurpolymj.2024.113551.

Data availability

Data will be made available on request.

References

[1] S. Correa, A.K. Grosskopf, H. Lopez Hernandez, D. Chan, A.C. Yu, L.M. Stapleton, E. A. Appel, Translational applications of hydrogels, Chem. Rev. 121 (2021) 11385–11457, https://doi.org/10.1021/acs.chemrev.0c01177.

[2] E.S. Dragan, Design and applications of interpenetrating polymer network hydrogels. A review, Chem. Eng. J. 243 (2014) 572–590, https://doi.org/10.1016/j.cej.2014.01.065.

[3] A.K. Gaharwar, N.A. Peppas, A. Khademhosseini, Nanocomposite hydrogels for biomedical applications, Biotechnol. Bioeng. 111 (2014) 441–453, https://doi.org/10.1002/bit.25160.

[4] J. Michalek, R. Hobzova, M. Pradny, M. Duskova, Hydrogels contact lenses, in: R. Ottenbrite, K. Park, T. Okano (Eds.), Biomedical Applications of Hydrogels Handbook, Springer, New York, 2010 pp.- 303–315.

[5] A. Kumar, K.M. Rao, S.S. Han, Synthesis of mechanically stiff and bioactive hybrid hydrogels for bone tissue engineering applications, Chem. Eng. J. 317 (2017) 119–131, https://doi.org/10.1016/j.cej.2017.02.065.

[6] Z. Han, P. Wang, G. Mao, T. Yin, D. Zhong, B. Yiming, X. Hu, Z. Jia, G. Nian, S. Qu, W. Yang, Dual pH-responsive hydrogel actuator for lipophilic drug delivery, ACS Appl. Mater. Interfaces 12 (2020) 12010–12017, https://doi.org/10.1021/acsami.9b21713.

[7] C.E. Kandow, P.C. Georges, P.A. Janmey, K.A. Beningo, Polyacrylamide hydrogels for cell mechanics: steps toward optimisation and alternative uses, Method Cell. Biol. 83 (2007) 29–46, https://doi.org/10.1016/S0091-679X(07)83002-0.

[8] J. Alipal, N.M. Pu'Ad, T.C. Lee, N.H.M. Nayan, N. Sahari, H. Basri, M.I. Idris, H. Z. Abdullah, A review of gelatin: Properties, sources, process, applications, and commercialisation, Mater. Today Proc. 42 (2021) 240–250, https://doi.org/10.1016/j.matpr.2020.12.922.

[9] A. Khalvandi, L. Tayebi, S. Kamarian, S. Saber-Samandari, J.I. Song, Data-driven supervised machine learning to predict the compressive response of porous PVA/Gelatin hydrogels and in-vitro assessments: employing design of experiments, Int. J. Biol. Macromol. 253 (2023) 126906, https://doi.org/10.1016/j.ijbiomac.2023.126906.

[10] S. Kalidas, S. Sumathi, Mechanical, biocompatibility and antibacterial studies of gelatin/polyvinyl alcohol/silkfibre polymeric scaffold for bone tissue engineering, Heliyon 9 (2023) 16886, https://doi.org/10.1016/j.heliyon.2023.e16886.

[11] G. Pagnotta, M. Becconi, M. Malferrari, D. Aiello, A. Napoli, L. Di Lisa, S. Grilli, S. Rapino, M.L. Focarete, Development of a tissue construct with spatially controllable stiffness via a one-step 3D bioprinting and dual-crosslinking process, Mater. Adv. 4 (2023) 3491–3505, https://doi.org/10.1039/D3MA00319A.

[12] K. Yue, G. Trujillo-de Santiago, M.M. Alvarez, A. Tamayol, N. Annabi, A. Khademhosseini, Synthesis, properties, and biomedical applications of gelatin methacryloyl (GelMA) hydrogels, Biomaterials 73 (2015) 254–271, https://doi.org/10.1016/j.biomaterials.2015.08.045.

[13] A. Serafim, C. Tucureanu, D.G. Petre, D.M. Dragusin, A. Salageanu, S. Van Vlierberghe, I.C. Stancu, One-pot synthesis of superabsorbent hybrid hydrogels based on methacrylamide gelatin and polyacrylamide. Effortless control of hydrogel properties through composition design, New J. Chem. 38 (2014) 3112–3126, https://doi.org/10.1039/c4nj00161c.

[14] L. Han, J. Xu, X. Lu, D. Gan, Z. Wang, K.H. Zhang, H. Yuan, J. Weng, Biohybrid methacrylated gelatin/polyacrylamide hydrogels for cartilage repair, J. Mater. J. Mater. Chem. B 5 (2017) 731–741, https://doi.org/10.1039/C6TB02348G.

[15] B.Z. Molino, C. O'Connell, T. Kageyama, L. Yan, Y. Wu, I. Kawamura, S. Maruo, J. Fukuda, Gelatin acrylamide with improved UV crosslinking and mechanical properties for 3D biofabrication, J. Biosci. Bioeng. 136 (2023) 51–57, https://doi.org/10.1016/j.jbiosc.2023.03.014.

[16] M. Abdallah, S. Nagarajan, M. Martin, M. Tamer, W.H. Faour, M. Bassil, F.J. C. Cuisiner, C. Gergely, B. Varga, O. Pall, P. Miele, S. Balme, M. El Tahchi, M. Bechelany, Enhancement of podocyte attachment on polyacrylamide hydrogels with gelatin-based polymers, ACS Appl. Bio Mater. 3 (2020) 7531–7539, https://doi.org/10.1021/acsabm.0c00734.

[17] Q. Li, H.X. Shen, C. Liu, C.F. Wang, L. Zhu, S. Chen, Advances in frontal polymerisation strategy: From fundamentals to applications, Prog. Polym. Sci. 127 (2022) 101514, https://doi.org/10.1016/j.progpolymsci.2022.101514.

[18] B.A. Suslick, J. Hemmer, B.R. Groce, K.J. Stawiasz, P.H. Geubelle, G. Malucelli, A. Mariani, J.S. Moore, J.A. Pojman, N.R. Sottos, Frontal polymerisations: from chemical perspectives to macroscopic properties and applications, Chem. Rev. 123 (2023) 3237–3298, https://doi.org/10.1021/acs.chemrev.2c00686.

[19] G. Malucelli, A. Mariani, Polymer hydrogels and frontal polymerization: a winning coupling, Polymers 15 (2023) 4242, https://doi.org/10.3390/polym15214242.

[20] D. Nuvoli, V. Alzari, L. Nuvoli, M. Rassu, D. Sanna, A. Mariani, Synthesis and characterisation of poly (2-hydroxyethylacrylate)/β-cyclodextrin hydrogels obtained by frontal polymerisation, Carbohydr. Polym. 150 (2016) 166–171, https://doi.org/10.1016/j.carbpol.2016.05.017.

[21] Q. Feng, X. Chen, Y.Q. Zhao, S.S. Hu, Z.W. Xia, Q.Z. Yan, Preparation of poly (N-isopropylacrylamide)/montmorillonite composite hydrogel by frontal polymerisation, Colloid Polym. Sci. 295 (2017) 883–890, https://doi.org/10.1007/s00396-017-4066-0.

[22] Q. Li, J.D. Liu, S.S. Liu, C.F. Wang, S. Chen, Frontal polymerisation-oriented self-healing hydrogels and applications toward temperature-triggered actuators, Ind. Eng. Chem. Res. 58 (2019) 3885–3892, https://doi.org/10.1021/acs.iecr.8b05369.

[23] N. Zoratto, P. Matricardi, Chapter 4, in: K. Pal, I. Banerjee (Eds.), Polymeric Gels, Woodhead Publishing, Sawston, 2018, pp. 91–124.

[24] E.S. Dragan, Advances in interpenetrating polymer network hydrogels and their applications, Pure Appl. Chem. 86 (2014) 1707–1721, https://doi.org/10.1515/pac-2014-0713.

[25] L. Xu, C. Wang, Y. Cui, A. Li, Y. Qiao, D. Qiu, Conjoined-network rendered stiff and tough hydrogels from biogenic molecules, Sci. Adv. 5 (2019) eaau3442, https://doi.org/10.1126/sciadv.aau3442.

[26] K. Razmjooee, A.R. Ahmady, N. Arabzadeh, S. Ahmadi, S. Saber-Samandari, D. Toghraie, Synthesis of Gelatin/Polyacrylamide/Carboxymethyl chitosan triple-network hydrogels and evaluation of their properties for potential biomedical applications, Mater. Sci. Eng. B 295 (2023) 116597, https://doi.org/10.1016/j.mseb.2023.116597.

[27] Z. Goudarzi, S. Saber-Samandari, Design and development of a novel multiple-network hydrogel composed of polyacrylamide, gelatin, and alginate as a wound dressing, Fibers Polym. 25 (2024) 3217–3228, https://doi.org/10.1007/s12221-024-00635-z.

[28] Y. Gan, P. Li, L. Wang, X. Mo, L. Song, Y. Xu, C. Zhao, B. Ouyang, B. Tu, L. Luo, L. Zhu, S. Dong, F. Li, Q. Zhou, An interpenetrating network-strengthened and toughened hydrogel that supports cell-based nucleus pulposus regeneration, Biomaterials 136 (2017) 12–28, https://doi.org/10.1016/j.biomaterials.2017.05.017.

[29] A. Mariani, L. Nuvoli, D. Sanna, V. Alzari, D. Nuvoli, M. Rassu, G. Malucelli, Semi-interpenetrating polymer networks based on crosslinked poly (N-isopropyl acrylamide) and methylcellulose prepared by frontal polymerisation, J. Polym. Sci., Part a: Polym. Chem. 56 (2018) 437–443, https://doi.org/10.1002/pola.28914.

[30] M. Rassu, V. Alzari, D. Nuvoli, L. Nuvoli, D. Sanna, V. Sanna, G. Malucelli, A. Mariani, Semi-interpenetrating polymer networks of methyl cellulose and polyacrylamide prepared by frontal polymerisation, J. Polym. Sci., Part A: Polym. Chem. 55 (2017) 1268–1274, https://doi.org/10.1002/pola.28498.

[31] V. Alzari, A. Ruiu, D. Nuvoli, R. Sanna, F.J. Jillescas-Martinez, D. Appelhans, B. Voit, S. Zschoche, A. Mariani, Three component terpolymer and IPN hydrogels with response to stimuli, Polymer 55 (2014) 5305–5313, https://doi.org/10.1016/j.polymer.2014.09.004.

[32] A. Martínez-Ruvalcaba, F. Becerra-Bracamontes, J.C. Sánchez-Díaz, A. González-Álvarez, Polyacrylamide-gelatin polymeric networks: effect of pH and gelatin concentration on the swelling kinetics and mechanical properties, Polym. Bull. 62 (2009) 539–548, https://doi.org/10.1007/s00289-008-0037-4.

[33] X. Yan, Q. Chen, L. Zhu, H. Chen, D. Wei, F. Chen, Z. Tang, J. Yang, J. Zheng, High strength and self-healable gelatin/polyacrylamide double network hydrogels, J. Mater. Chem. B 5 (2017) 7683–7691, https://doi.org/10.1039/C7TB01780D.

[34] W. Fan, Z. Zhang, Y. Liu, J. Wang, Z. Li, M. Wang, Shape memory polyacrylamide/gelatin hydrogel with controllable mechanical and drug release properties potential for wound dressing application, Polymer 226 (2021) 123786, https://doi.org/10.1016/j.polymer.2021.123786.

[35] B. Lv, X. Bu, Y. Da, P. Duan, H. Wang, J. Ren, B. Liu, D. Gao, J. Ma, Gelatin/PAM double network hydrogels with super-compressibility, Polymer 210 (2020) 123021, https://doi.org/10.1016/j.polymer.2020.123021.

[36] H. Shirahama, B.H. Lee, L.P. Tan, N.J. Cho, Precise tuning of facile one-pot gelatin methacryloyl (GelMA) synthesis, Sci. Rep. 6 (2016) 31036, https://doi.org/10.1038/srep31036.

[37] R. Leu Alexa, A. Cucuruz, C.D. Ghițulică, G. Voicu, L.R. Stamat, S. Dinescu, G. M. Vlasceanu, C. Stavarache, R. Ianchis, H. Iovu, M. Costache, 3D printable composite biomaterials based on GelMA and hydroxyapatite powders doped with cerium ions for bone tissue regeneration, Int. J. Mol. Sci. 23 (2022) 1841. https://www.mdpi.com/1422-0067/23/3/1841.

[38] D. Nečas, P. Klapetek, Gwyddion: an open-source software for SPM data analysis, Cent. Eur. J. Phys. 10 (2012) 181–188, https://doi.org/10.2478/s11534-011-0096-2.

[39] R. Böttger, L. Bischoff, S. Facsko, B. Schmidt, Quantitative analysis of the order of Bi ion induced dot patterns on Ge, Europhys. Lett. 98 (2012) 16009, https://doi.org/10.1209/0295-5075/98/16009.

[40] F. Valle, M. Brucale, S. Chiodini, E. Bystrenova, C. Albonetti, Nanoscale morphological analysis of soft matter aggregates with fractal dimension ranging from 1 to 3, Micron 100 (2017) 60–72, https://doi.org/10.1016/j.micron.2017.04.013.

[41] N.D. Petkovich, A. Stein, B.L. Su, C. Sanchez, X.Y. Yang, Chapter 5, in: B.L. Su, C. Sanchez, X. Yang, (Eds.), Hierarchically Structured Porous Materials: From Nanoscience to Catalysis, Separation, Optics, Energy and Life Science, Wiley, Hoboken, 2012, pp. 131–172.